

Liquid Water Content and Temperature Relationship from Aircraft Observations and Its Applicability to GCMs

I. GULTEPE AND G. A. ISAAC

Atmospheric Environment Service, Cloud Physics Research Division, Downsview, Ontario, Canada

(Manuscript received 1 September 1995, in final form 22 July 1996)

ABSTRACT

The vertical distribution of liquid water content (LWC) and its relationship with temperature (T) strongly affect the heat budget of the atmosphere. Some large-scale models of the atmosphere use a relationship between LWC and T to diagnostically obtain LWC from T under saturated conditions. Airborne observations conducted within clouds over northeastern North America during the 1984–93 time period are used to study the relationship between LWC and T. Observed frequency distributions of LWC are approximated by lognormal distribution curves and are best represented by median values. The median LWC values monotonically increase with warmer temperatures. However, the mean LWC reaches 0.23 g m^{-3} at about $T = 2.5^\circ\text{C}$. LWC decreases below and above 2.5°C , except that it reaches a maximum value of 0.26 g m^{-3} at 22.5°C . The relationship between LWC and T from the present study is compared with that of earlier studies from the former Soviet Union. Differences can be attributed to the design and limits of the probes, natural variability in the 35 years, and the limited dataset for some temperature intervals. The LWC versus T relationship developed from observations in this study can be compared with large-scale model simulations.

1. Introduction

Clouds formed by different physical and dynamical processes, and with different aerosol characteristics, play an important role in climate change and the general circulation of the atmosphere. Understanding the physical and dynamical structures of clouds is strongly dependent on how well liquid water content (LWC) and ice water content (IWC) profiles are known in the atmosphere.

Liquid water content is an important parameter that influences the dynamical structure and radiative characteristics of clouds (Gultepe and Rao 1993; Browning 1994; McFarlane et al. 1992). Furthermore, it is a crucial parameter that can be related to other parameters (i.e., radiative absorption, optical thickness) within GCMs (Slingo and Schrecker 1982). Liou and Ou (1989) used an LWC–temperature (T) relationship from Feigelson (1978) for comparison with 1D climate model results. Smith (1990), on the other hand, used a LWC–T relationship based on a quadratic spline. He stated that the form of his relationship has no basis in observation and theory. Based on model-derived T and using an adiabatic assumption, LWC was estimated from thermodynamic relations by Betts and Harshvardhan (1987).

But there were no detailed observations other than Feigelson (1978) for comparison to their study. Although there are many field projects around the globe, there is no complete database that can be used for LWC analysis.

For this reason, aircraft observations from several Canadian field projects (1984–93) were used to characterize the LWC–T relationship for northern latitudes. These observations are compared with measurements made in the former Soviet Union, which are widely used by the modeling community.

2. LWC probes

This paper describes measurements made using three different LWC probes. The Canadian data were obtained using a King probe, while the studies from the former Soviet Union used Zaitsev and Nevzorov probes. A brief description of each device is given in this section.

The earlier probes measuring LWC (e.g., Johnson–Williams probe) underestimate the mass of droplets with diameters greater than about $30 \mu\text{m}$ and have a poor response to precipitation size drops (Knollenberg 1972). Partly because of this, King et al. (1978, 1981) developed a hot-wire liquid water probe, which requires a simple dry calibration and has a sensitivity of about 0.02 g m^{-3} with a response time of 0.05 s and an accuracy of about 5% at 1 g m^{-3} . King probe observations can have large uncertainty when the droplet diameter is greater than $50 \mu\text{m}$ (King et al. 1981).

LWC measurements from aircraft in the former Soviet

Corresponding author address: Dr. Ismail Gultepe, Cloud Physics Research Division, Atmospheric Environment Service, 4905 Dufferin Street, Downsview, ON M3H-5T4 Canada.
E-mail: ismail@armph3.dow.on.doe.ca

TABLE 1. Field experiments used in the analysis. The entire dataset from the field projects lies between -30°C and 25°C .

Experiment	Year	Period	Location [lat; long]	T range [$^{\circ}\text{C}$]
Syracuse	1984	17 Oct–14 Nov	43:04°N 76:11°W	[−15; 15]
EMEFS I	1988	21 Jul–29 Aug	44:58°N 79:18°W	[−10; 20]
EMEFS II	1990	20 Mar–29 Apr	46:20°N 79:30°W	[−10; 10]
CASP II	1992	15 Jan–15 Mar	47:35°N 52:40°W	[−30; 5]
NARE	1993	6 Aug–8 Sep	43:50°N 65:30°W	[0; 20]

Union have been described in many papers (e.g., Zaitsev 1950; Borovikov et al. 1963), which were obtained with a Zaitsev probe that uses filter paper as the detection medium. Mazin (1995) reports on measurements from this device made from 31 aircraft sounding network stations during the period of 1957–63. At temperatures colder than 0°C , a threshold value LWC of 0.032 g m^{-3} was used, while at temperatures warmer than 0°C , the threshold was 0.05 g m^{-3} (Borovikov et al. 1963). Feigelson (1978) used these measurements, and his results showed that the LWC values reported differ by $\pm 0.01\text{ g m}^{-3}$ from the values given by Mazin (1995). Because of low ice water content values at about -40°C , this difference can be important at cold temperatures.

The Nevzorov probe was developed in the 1970s. This probe is based on a modification of the hot-wire technique (Nevzorov 1980; Nevzorov and Shugaev 1992). The threshold of this probe is given as 0.003 g m^{-3} . It has a capability of measuring particles between $5\text{ }\mu\text{m}$ and 8 mm (Mazin et al. 1992). The probe consists of sensors that measure LWC and total condensate content (TCC), that is, water from both droplets and ice particles. The uncertainty in the Nevzorov probe is not larger than 10% (Nevzorov 1980; Mazin 1995). The accuracy of this probe depends on knowledge about the response characteristics and collision efficiencies. Based on statistical processing of data, a correction factor for the LWC is suggested by Mazin (1995) that ranges from 1 at temperatures warmer than 0°C to 1.3 at -35°C .

3. Observations

Observations from five field projects are used in this study: the North Atlantic Regional Experiment (NARE), the Canadian Atlantic Storm Program (CASP II), the Eulerian Model Evaluation Field Studies (EMEFS I and II), and the Syracuse field study. Cloud systems, which were sampled almost randomly in location and time, were composed of largely thin and thick stratiform clouds. The maximum height of cloud top was usually less than 7 km and the cloud base was usually greater than a few hundred meters. Droplet number concentrations within stratus clouds during the CASP II and NARE projects, which were conducted in eastern Canada, indicate both continental and maritime type clouds. The other projects sampled clouds in the middle of the North American continent.

The approximate location, temperature range, cloud type, and dates for each project are shown in Table 1.

The National Research Council of Canada DHC-6, Twin Otter, or Convair-580 aircraft were used to collect data. Detailed information about observations during these projects can be found elsewhere [NARE, Leitch et al. (1994); CASP II, Cober et al. (1995); EMEFS I and II, Isaac et al. (1992); and Syracuse, Gillani et al. (1995); Isaac et al. (1990)].

Although there are several other observations from the projects related to the microphysical, radiation, and dynamical characteristics of these clouds, the main data used for this study were LWC, T, and pressure (P). Observations averaged for 1 s are used. A reverse flow probe was used to measure T, with an error of approximately $\pm 1^{\circ}\text{C}$. A Paroscientific 215L probe or Rosemount 858 5-hole pressure probe measured P. As stated above, the LWC was obtained using a PMS King probe that has uncertainty less than 0.02 g m^{-3} (King et al. 1978). During CASP II, the data were removed from the analysis if the PMS cloud droplet measuring probe (FSSP) showed droplet number concentration (N_d) less than 10 cm^{-3} . This cutoff limit helped remove measurements that could be contaminated by ice crystals. Cober et al. (1995) have indicated that the King probe LWC values can be contaminated up to 15% by ice crystals. For other projects, the lower limit for N_d was chosen as 2 cm^{-3} .

The field studies (Mazin 1995) used for comparisons represent aircraft observations during 1) the period of 1957–63 (Borovikov et al. 1963; Feigelson 1978; Matveev 1984), and 2) the period of 1978–84 (Nevzorov 1980; Ataman et al. 1992). During the former period, LWC measurements from the Zaitsev probe were filtered and used if larger than 0.032 g m^{-3} at temperatures less than 0°C , and 0.05 g m^{-3} at temperatures greater than 0°C (Borovikov et al. 1963). The Nevzorov probe detection threshold for the later period was given as 0.003 g m^{-3} . Observations used in the Mazin study represent the entire territory of the former Soviet Union, and all kinds of clouds are used in their analysis.

4. Analysis and results

Statistical and physical relationships between T and LWC have been given in a few previous studies (Mazin and Shmeter 1983; Feigelson 1978; Liou and Ou 1989; Gultepe et al. 1996). For this study, LWC data are classified into 5°C temperature intervals between -30° and 25°C . Table 2 shows the number of data points and mean and standard deviation (sd) of P and LWC per temper-

TABLE 2. Shows the number of points that fall into temperature intervals and mean and standard deviation (sd) of pressure and LWC.

T Range [°C]	# of Points	\bar{P}/sd [mb]	\bar{LWC}/sd [$g\ m^{-3}$]
-30; -25	4503	526.3/92.3	0.044/0.035
-25; -20	2017	627.0/123.5	0.080/0.103
-20; -15	6617	720.9/132.1	0.074/0.071
-15; -10	18 654	778.2/137.6	0.088/0.090
-10; -5	29 586	789.8/139.9	0.113/0.133
-5; 0	63 867	818.9/114.7	0.127/0.119
0; 5	31 674	816.4/113.0	0.228/0.328
5; 10	10 461	802.4/87.3	0.194/0.184
10; 15	25 409	865.6/67.7	0.205/0.165
15; 20	12 175	931.2/55.4	0.167/0.148
20; 25	5418	941.9/38.6	0.262/0.157

TABLE 3. Percentiles of LWC distribution, median LWC (LWC_m), and standard deviation (σ) of $\log(LWC)$. LWC is greater than $0.01\ g\ m^{-3}$.

T [°C] Range	20%	80%	95%	LWC_m	$\sigma_{\log(LWC)}$
-25; -30	0.014	0.065	0.13	0.037	0.344
-20; -25	0.02	0.10	0.27	0.043	0.410
-15; -20	0.02	0.11	0.22	0.048	0.394
-10; -15	0.023	0.13	0.24	0.059	0.400
-5; 10	0.028	0.18	0.27	0.07	0.430
0; 5	0.03	0.195	0.31	0.08	0.428
5; 0	0.05	0.22	0.38	0.12	0.454
10; 5	0.045	0.25	0.40	0.15	0.445
15; 10	0.043	0.27	0.46	0.13	0.458
20; 15	0.06	0.23	0.46	0.17	0.426
25; 20	0.12	0.35	0.53	0.20	0.303

ature interval. The frequency of LWC occurrence within a $5^\circ C$ temperature interval range is approximated by distribution curves. The median and various percentile values of LWC are estimated from the cumulative frequency distribution. In addition to the LWC-T relationship, a relationship among LWC, T, and P is also derived, because the profile of LWC as a function of T and P can be obtained from the general circulation models.

Figure 1 shows the cumulative frequency values of $LWC > 0.01\ g\ m^{-3}$ for each temperature range or bin of Table 2. In calculations for each temperature bin,

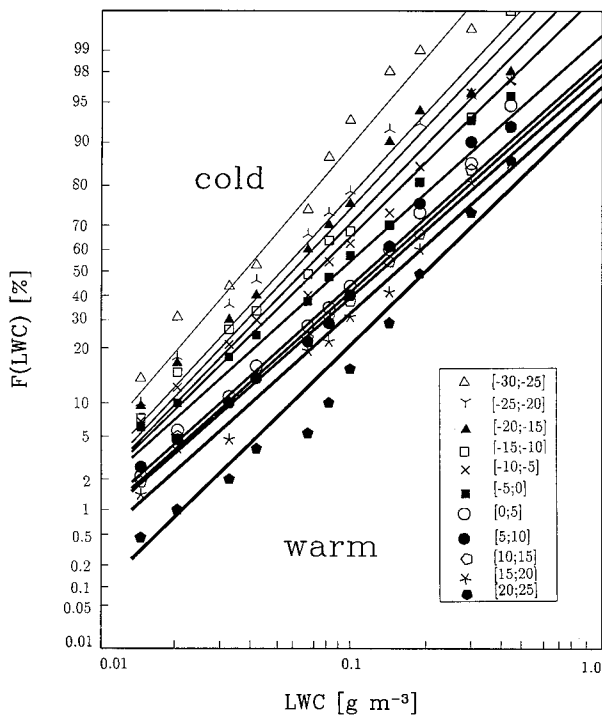


FIG. 1. The cumulative frequency distribution of LWC for T intervals. The symbols representing temperature intervals are shown in the inner panel. The lines from light to dark correspond to cold to warm. The LWC is greater than $0.01\ g\ m^{-3}$.

measurements of $\log(LWC)$ are binned into 30 intervals of width 0.1 spanning liquid water contents between $10^{-2}\ g\ m^{-3}$ and $1\ g\ m^{-3}$. The lines from light to dark correspond from cold to warm. The symbols representing T intervals are shown in the inner panel. Selected percentiles and median values of LWC, and standard deviation (σ) obtained are shown in Table 3.

The relationship between the mean LWC (\bar{LWC}) and T is shown in Fig. 2. The second-order polynomial fits to data is shown with the dash-dot line, and its equation is given in Table 4 [Eq. (1)]. An increase in LWC around $0^\circ C$ might result from melting processes.

Other curve fits are shown in Table 4. Equation (2) shows the relationship between mean LWC, T and P; Eqs. (3) and (4) show linear regressions of \bar{LWC} -T and median LWC (LWC_m)-T with LWC being in units of g

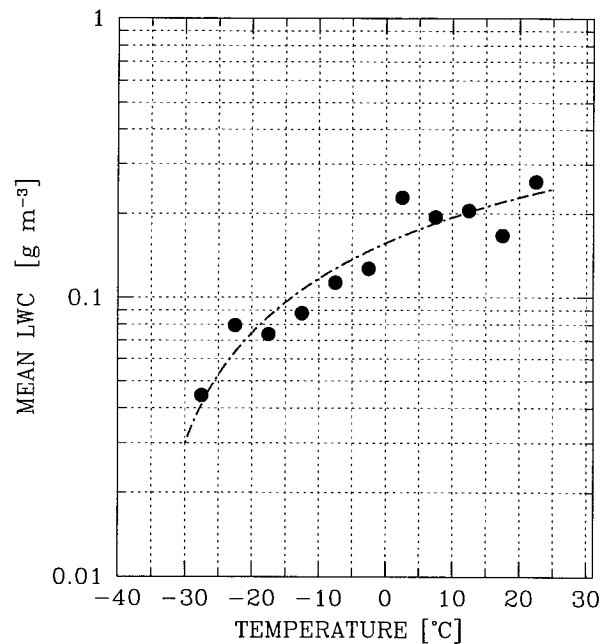


FIG. 2. Mean LWC versus T. The dash-dot line represents the second power polynomial fit (Table 4).

TABLE 4. Relationships obtained from observations. Here, \overline{LWC} , T, and pressure (P) have the units of $g\ m^{-3}$, $^{\circ}C$, and mb, respectively, except for Eq. (5) where LWC is in $g\ kg^{-1}$. Here, R shows the correlation coefficient. Subscript *m* indicates median values.

Relationship	R	Eq.
$\log(\overline{LWC}) = -1.24942e-05T^2 + 0.00384298T + 0.156445$	—	1
$\log(LWC) = -1.076 + 0.01171T + 0.0002625P$	0.86	2
$\log(LWC) = -0.8646 + 0.01359T$	0.93	3
$\log(LWC_m) = -1.02430 + 0.01568T$	0.98	4
$\log(LWC_m) = -0.48911 + 0.01344T$	0.96	5

m^{-3} . The analysis was also repeated converting LWC into units of $g\ kg^{-1}$, and Eq. (5) of Table 4 shows the resulting relationship. A 2%–13% error in LWC occurs when a constant pressure value is assumed in Eq. (2) of Table 4.

Cumulative values of LWC occurrence [F(W)] as a function of a normalized variable *t* [$\log(LWC) - \log(LWC_m)/\sigma$] for each T interval are shown in Fig. 3 where observations are found between the dashed and fitted lines. The best fit curves are drawn assuming a lognormal distribution with specified median and standard deviation values. As seen in Fig. 3, that large uncertainty occurs in the lower and higher probability values. Standard deviation (σ) is obtained from $\log(LWC)$ values at each temperature interval. The difference between the distribution curves and the observations become important at the lower limits of LWC for each T interval. The higher correlation coefficient using median values in comparison to arithmetic averages (see Table 4) shows the value of the lognormal approximation suggested by Mazin (1995).

The 20%, 50%, 80%, and 95% percentile values of the LWC cumulative distribution curves are shown in

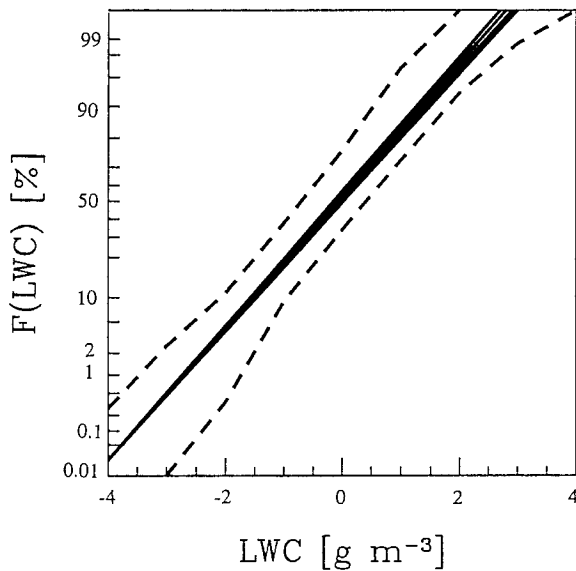


FIG. 3. The normalized cumulative frequency distribution line, which is obtained by using equations given in Table 4. Dashed lines are outer limits for the observations. Solid lines are for each T interval given in Table 2.

Fig. 4. The solid circles represent the median values at a given T interval and the dashed line is the best fit represented by Eq. (4) (Table 4). The values of LWC in Fig. 4 increase with increasing temperature and percentile values. The increase in LWC seen near $0^{\circ}C$ in Fig. 2 is not evident in Fig. 4.

5. Discussion

The present study contains 211 000 data points, each representing 1 s (0.07–0.10 km of pathlength). As mentioned before, the Mazin (1995) study consisted of two periods. The first period (1960s) covers 20 000 data points, approximately, and these data were also used by Feigelson (1978). The second period contains 145 000 data points with each averaged over a 5-s interval (0.6–0.7 km pathlength). The Moss and Johnson (1993) study used about 10 000 data points, each representing 1 s (about 0.1 km pathlength). Consequently, the present study is one of the largest datasets analyzed. The results of the present study also represent a larger extended time period (9 years vs 6 years) and, as Fig. 5 shows, document LWC values at warmer temperatures than before.

Scale length is an important issue. Table 5 shows the NARE data analyzed using 1-s, 50-s, and 500-s aver-

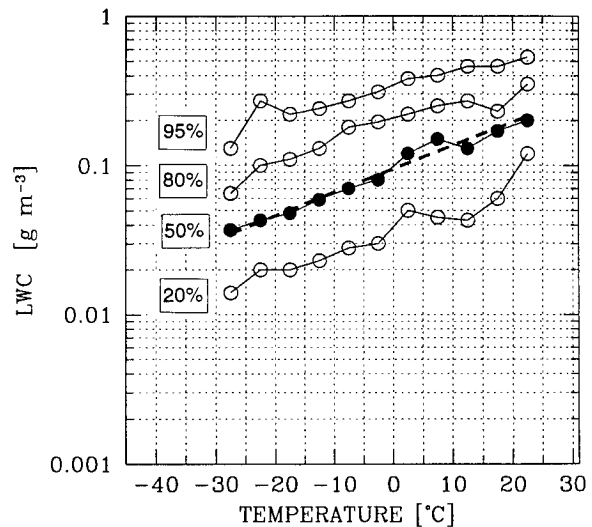


FIG. 4. LWC vs T for given percentile values. Filled circles are for median values and dashed line is for best fit to data.

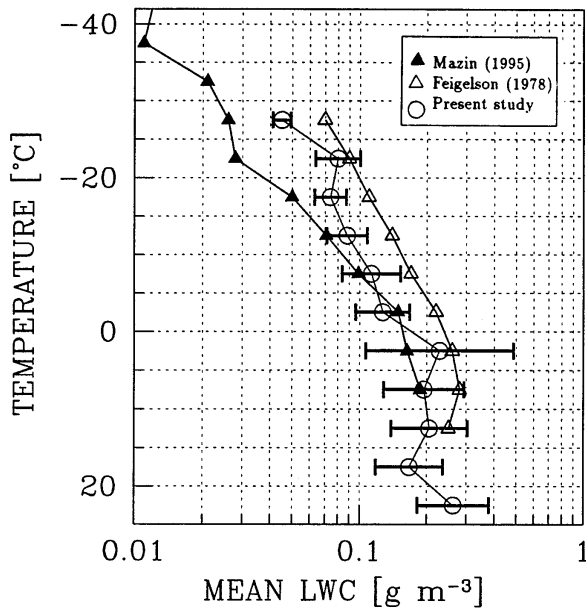


FIG. 5. Profiles of mean LWC: the line with black triangles is from Feigelson (1978), the line with filled triangles from Mazin (1995), and the line with blank circles from Canadian observations. The bars indicate the standard deviation for the Canadian observations (Table 2).

aging intervals. This corresponds to scale lengths of 75 m, 3.8 km, and 38 km. Average values less than 0.01 g m^{-3} were removed from the analysis. The data were then put into temperature bins in a similar manner to the analysis performed for Table 2. Table 5 clearly shows decreasing values with increasing averaging interval. The LWC threshold value of 0.01 g m^{-3} will reject more individual averages from the longer averaging intervals. In addition, since clouds are often patchy, the longer averaging intervals contain cloud-free periods, which artificially reduces LWC. This helps explain some of the differences seen in Table 5, but it also indicates that selection of an averaging interval is not a simple task. Because the data are put into 5°C bins before averages are obtained, it would be difficult to assign an actual scale length to the results of Table 4. It is also not obvious how data should be analyzed to make them more useful for comparison to large-scale models, which use grid lengths usually greater than 50 km. Certainly, Cotton et al. (1995) have recognized this scale problem and the challenge it represents.

Figure 5 shows the mean LWC versus temperature profiles from the Canadian, Mazin (1995), and Feigelson (1978) observations. In this figure, mean LWC values of the present study increase from 0.04 g m^{-3} at -27.5°C to 0.23 g m^{-3} at 2.5°C . Then, LWC starts to decrease until T reaches 17.5°C . At the lowest altitude, the maximum LWC of 0.26 g m^{-3} is found at about 22.5°C . Mean LWC values at 22.5°C were not available from other studies. In that respect, the maximum value at the highest T can be explained only by limited and biased observations with respect to time and location.

TABLE 5. Mean and standard deviation of 1-s, 50-s, and 500-s averaged LWC data for 5°C T intervals during NARE. The final column indicates the number of 1-s values used.

T [$^\circ\text{C}$]	LWC ¹ /sd [g m^{-3}]	LWC ⁵⁰ /sd (g m^{-3})	LWC ⁵⁰⁰ /sd [g m^{-3}]	# of points
0–5	0.046/0.063	0.068/0.087	0.020/0.001	258
5–10	0.176/0.194	0.100/0.117	0.079/0.074	1962
10–15	0.189/0.105	0.167/0.110	0.126/0.089	12 680
15–20	0.139/0.114	0.105/0.104	0.060/0.061	8339
20–25	0.261/0.157	0.253/0.152	0.214/0.080	5345
mean/sd	0.16/0.13	0.14/0.11	0.10/0.06	

It can be seen from Table 1 that most of the LWC values at that temperature come from the NARE project, which represents clouds over ocean. Therefore, mean LWC at the lowest altitude (Table 2) may include a large uncertainty.

The values of the Mazin study using 1980s data are significantly smaller than the Feigelson study, which used 1960s data (Fig. 5). On the other hand, the present values are comparably larger than the Mazin study, especially at colder temperatures. The Mazin data includes the sum of ice and liquid observations together. At colder temperatures, there is probably more ice than liquid present in the clouds. Consequently, if the Mazin data were changed to remove the measurements in which ice crystals were present, the differences between his values and the present values at colder temperatures would probably change, although the magnitude or direction of that change is difficult to assess.

The detection limits for each of the datasets also play an important role in the LWC– T relationship and help explain some of the differences seen in Fig. 5. The Feigelson data tend to be larger than the present observations, and our observations are greater than those of Mazin, which follows the differences in detection limits of 0.032 g m^{-3} , 0.01 g m^{-3} , and 0.003 g m^{-3} , respectively. Mazin stressed the importance of the detection limits in any comparison of datasets, and this study provides support to his arguments.

There is also no intercomparison or similar calibration of the Zaitsev, Nevzorov, and King probes, which would have been very useful and might have helped explain the differences seen in Fig. 5. Another reason for the difference between the results is likely due to natural variability of clouds over a 30-yr time period.

Two earlier studies (Smith 1990; Moss and Johnson 1994) stated that no liquid water content was found for $T < -15^\circ\text{C}$. This is a contradiction to the data presented here. LWC in the present study is found between $-30^\circ\text{C} < T < -25^\circ\text{C}$ in 4500 samples. Mateev (1984) and Heymsfield (1993) also found liquid water at $T < -15^\circ\text{C}$.

The ratio of LWC versus TCC, f_l , is a significant parameter for GCM applications. Table 6 shows the f_l from different studies. A simple approach to separate liquid from ice is given by Smith (1990). His equations

TABLE 6. The parameterized equations used in climate models. The third column indicates the temperature where no LWC is present. Note that number of data points N_p used for obtaining each equation is less than that of present study.

Author	Equation	100% icing at	T range	Based on	$\approx N_p$
Smith (1990)	$f_i = 1/6[(T + 15)/5]^2$	-15	-15:-5	—	—
Smith (1990)	$f_i = 1 - (1/3)[T/5]^2$	—	-5:0	—	—
Moss and Johnson (1994)	$f_i = 0.095T + 0.86$	-10	-10:5	1993 data	10 000
Rockel et al. (1991)	$f_i = 0.0059 + 0.9941e^{-0.003102T^2}$	-45	-50:0	1960 data	20 000
Sun (1995)	$f_i = 0.0059 + 0.8784e^{-0.005457T^2}$	-55	-50:0	1960 data	20 000

do not have much physical basis, because many observations indicated that LWC can be found at temperatures close to -40°C . This result is also indicated by the present study.

For mixed phase clouds, a relationship based on a 2D-C probe measurements from aircraft is given by Moss and Johnson (1994). The upper temperature limit for their equation is about -10°C , below which clouds become totally glaciated. Ice crystals with sizes less than $125\ \mu\text{m}$ were not included in their study. Based on the Matveev (1984) study, which used 1960s aircraft observations in the former Soviet Union, mixed phase clouds can exist in a large temperature range. His results are based on the frequency of cloud phase appearance, and are totally different than the studies of Moss and Johnson, and Smith.

Using Matveev's data, Rockel et al. (1991) suggested an equation given in Table 6. Sun (1995) reconsidered Matveev's results as shown by Rockel et al. and his results are based on LWC fraction of TCC rather than frequency. This equation is valid for T less than 0°C . Complete icing occurs at $T = -45^\circ\text{C}$ and $T = -55^\circ\text{C}$ for the Rockel et al. (1991) and Sun (1995) studies, respectively. The most important problem with the Rockel et al. and Sun studies is that they used 1960s data with a detection limit up to $0.05\ \text{g m}^{-3}$. Also, the instruments used to collect the data in the 1960s were not calibrated with up-to-date standards, and they have not been compared with present instruments. Filtering data at about $0.05\ \text{g m}^{-3}$ probably represents the most important error source.

Data from Heymsfield (1993), who obtained ice water content (IWC) observations from clouds over Wisconsin, and the present observations can be qualitatively compared to the values of f_i given in Table 6. Data from the Heymsfield study and the present one represent similar large-scale characteristics of the atmosphere and geographical location. The Canadian data were collected in low-level clouds, while Heymsfield studied cirrus clouds. Comparisons of these datasets, and other earlier studies, suggest that f_i cannot be zero at temperatures near -10 to -15°C . Further work will be required to quantify the f_i relationship with temperature.

6. Conclusions

This study used a large dataset from field projects, which took place over Canada and the USA during the

period of 1984–93. Each field experiment was made for the study of various physical, chemical, dynamical, and radiative processes occurring within the cloud or the cloud-free environment. Because of the interest of climate/weather modelers regarding the LWC distribution in the vertical within clouds, the observations were analyzed to obtain an LWC–T relationship. For each temperature interval, LWC frequency values were approximated by a lognormal distribution curve. This indicated the mode of the distribution would be best represented by the median value, rather than an arithmetic average. Figure 4 shows the best summary of this data.

The LWC profile from model results of Liou and Ou (1989) were found to be much closer to the result of this study compared to Feigelson (1978). The present study indicates an overestimation of LWC with a maximum about $0.1\ \text{g m}^{-3}$ in his work. This difference is likely due to the threshold value used in the LWC calculation rather than cloud type. Convective clouds included in his work represent only 2% of all the clouds. In addition, McFarlane et al. (1992) used the Betts and Harshvardhan (1987) study and Feigelson (1978) data for specifying LWC distributions in their cloud scheme. The Betts and Harshvardhan (1987) study uses an adiabatic assumption. However, the Canadian observations, and those of many others, indicated that cloud LWC rarely approaches adiabatic values. It is obvious that better estimates of LWC in climate models require improved comparisons with observations.

Satellite data from SSM/I sensors obtain vertically integrated LWC amounts that can be used for comparisons with models (Greenwald et al. 1995). These sensors provide global coverage but lack resolution in the vertical. However, very few studies have actually compared the data from these sensors to in situ measurements obtained from aircraft (e.g., Cober et al. 1996). It would be preferable to combine data from aircraft, ground based sensors such as microwave radiometers, and satellite systems to obtain datasets for comparison with models.

The data used in this study showed a large variability in LWC versus T. The data best represent conditions over northeastern North America. Also, the former Soviet Union observations do not represent conditions for the entire world. For these reasons, archived data from other parts of the world should be integrated together to get a more accurate LWC–T relationship. Because of

the lack of information on the ice phase, more measurements are also required to better evaluate the f_i versus T relationship. This information is crucial for the development and evaluation of climate and weather forecasting models.

Acknowledgments. The authors would like to thank M. Couture and D. Kellow of the Cloud Physics Research Division of the Atmospheric Environment Service (AES) for assistance in the data analysis. The authors are also grateful to I. MacPherson of the National Research Council (NRC) of Canada and S. Bacic of AES for data-related discussions. This analysis would not be possible without getting help from several key people during five different field projects, including J. W. Strapp, S. Cober, W. R. Leitch, and A. Korolev. The aircraft data were obtained with the assistance of the NRC.

REFERENCES

- Ataman, A. V., S. N. Burkovskaya, E. T. Ivanova, I. P. Mazin, and V. F. Shugaev, 1992: Arkhiv LFO CAO-Samoletnye izmerenia pokazatelja oslablenija vidimogo sveta i wodnosti oblakov. *Tr. CAO*, **180**, 34–42.
- Betts, A. K., and Harshvardhan, 1987: Thermodynamic constraint on the cloud liquid water feedback in climate models. *J. Geophys. Res.*, **92**, 8483–8485.
- Borovikov, A. M., I. I. Gaivoronskii, V. V. Kostarev, I. P. Mazin, V. E. Minervin, A. K. Khrgian, and S. M. Shmeter, 1963: *Cloud Physics*. Israel Program for Scientific Translations, 392 pp.
- Browning, K. A., 1994: Survey of perceived priority issues in the parameterization of cloud-related processes in GCMs. *Quart. J. Roy. Meteor. Soc.*, **120**, 483–487.
- Cober, S. G., G. A. Isaac, and J. W. Strapp, 1995: Aircraft icing measurements in east coast winter storms. *J. Appl. Meteor.*, **34**, 88–100.
- , J. W. Strapp, and G. A. Isaac, 1996: Comparisons of SSM/I liquid water paths with aircraft measurements. *J. Appl. Meteor.*, **35**, 503–519.
- Cotton, W. R., B. Stevens, and S. Nebuda, 1995: A question of balance simulating microphysics and dynamics. Preprints, *Conf. on Cloud Physics*, Dallas, TX, Amer. Meteor. Soc., 484–486.
- Feigelson, E. M., 1978: Preliminary radiation model of a cloudy atmosphere. Part I: Structure of clouds and solar radiation. *Beitr. Phys. Atmos.*, **51**, 203–229.
- Gillani, N. V., W. R. Leitch, J. W. Strapp, and G. A. Isaac, 1995: Field observations in continental stratiform clouds: Partitioning of cloud particles between droplets and unactivated interstitial aerosols. *J. Geophys. Res.*, **100**, 18 687–18 706.
- Greenwald, T. J., G. L. Stephens, S. A. Christopher, and T. H. Vonder Haar, 1995: Observations of the global characteristics and regional radiative effects of marine cloud liquid water. *J. Climate*, **8**, 2928–2946.
- Gultepe, I., and G. V. Rao, 1993: Moisture and heat budget of a cirrus cloud from aircraft measurements during FIRE. *Quart. J. Roy. Meteor. Soc.*, **119**, 957–974.
- , G. Isaac, R. Leitch, and C. M. Banic, 1996: Microphysical parameterization of aircraft observations collected during the NARE: Implications for GCMs. *J. Climate*, **9**, 345–357.
- Heymsfield, A. J., 1993: Microphysical structures of stratiform and cirrus clouds. *Aerosols-Cloud-Climate Interactions*, P. V. Hobbs, Ed., Academic Press, 97–121.
- Isaac, G. A., W. R. Leitch, and J. W. Strapp, 1990: The vertical distribution of aerosols and acid related compounds in air and cloud water. *Atmos. Environ.*, **24**(A), 3033–3046.
- , and Coauthors, 1992: Daytime and nighttime vertical profiles of atmospheric aerosols and trace gases during the intensive measurement periods of EMEFS. *Precipitation Scavenging and Atmosphere-Surface Exchange Processes*, S. E. Schwartz and W. G. N. Slinn, Eds., Hemisphere Publications, 1485–1496.
- King, W. D., D. A. Parkin, and R. J. Handsworth, 1978: A hot-wire liquid water device having fully calculable response characteristics. *J. Appl. Meteor.*, **17**, 1809–1813.
- , C. T. Maher, and G. A. Hepburn, 1981: Further performance tests on the CSIRO liquid water probe. *J. Appl. Meteor.*, **20**, 195–202.
- Knollenberg, R. E., 1972: Comparative liquid water content measurements of conventional instruments with an optical array spectrometer. *J. Appl. Meteor.*, **11**, 501–508.
- Leitch, W. R., and Coauthors, 1994: Aerosol particle and cloud droplet measurements during the 1993 North Atlantic Regional Experiment. Proc. *Conf. on Atmospheric Chemistry*, Nashville, TN, Amer. Meteor. Soc., 21–26.
- Liou, K. N., and S. C. Ou, 1989: The role of cloud microphysical processes in climate: An assessment from a one-dimensional perspective. *J. Geophys. Res.*, **94**, 8599–8607.
- Matveev, L. T., 1984: *Cloud Dynamics*. D. Reidel, 340 pp.
- Mazin, I. P., 1995: Cloud water content in continental clouds of middle latitudes. *J. Atmos. Res.*, **35**, 283–297.
- , and S. M. Shmeter, 1983: Oblaka: Stroenie i efizika obrazovaniya. *Gidrometeoizdat*, 279 pp.
- , A. N. Nevzorov, V. F. Shugaev, and A. V. Korolev, 1992: Phase structure of stratiform clouds. Preprints, *11th Int. Conf. on Clouds and Precipitation*, Montreal, PQ, Canada, Amer. Meteor. Soc., 332–335.
- McFarlane, N. A., G. J. Boer, J. -P. Blanchet, and M. Lazare, 1992: The Canadian Climate Center second generation general circulation model and its equilibrium climate. *J. Climate*, **5**, 1013–1044.
- Moss, S. J., and D. W. Johnson, 1994: Aircraft measurements to validate and improve numerical model parameterizations of ice to water ratios in clouds. *Atmos. Res.*, **34**, 1–25.
- Nevzorov, A. N., 1980: Aircraft cloud water content meter. Preprints, *Comm. a la 8eme Conf. Int. sur la Physic des Nuages*, AIMPA, Clermont-Ferrand, France, 701–703.
- , and V. F. Shugaev, 1992: Observations of the initial stage of ice phase evolution in supercooled clouds. *Soviet Meteor. Hydrol.*, **1**, 69–76.
- Rockel, B., E. Raschke, and B. Weyres, 1991: A parameterization of broad band radiative transfer properties of water, ice, and mixed clouds. *Beitr. Phys.*, **64**, 1–12.
- Slingo, A., and H. M. Schrecker, 1982: On the shortwave radiative properties of stratiform water clouds. *Quart. J. Roy. Meteor. Soc.*, **108**, 407–426.
- Smith, R. N. B., 1990: A scheme for predicting layer clouds and their water content in a general circulation model. *Quart. J. Roy. Meteor. Soc.*, **116**, 407–426.
- Sun, Z., 1995: Comparison of observed and modeled radiation budget over the Tibetan plateau using satellite data. *Int. J. Climatol.*, **15**, 423–445.
- Zaitsev, V. A., 1950: Vodnost' i raspredelenie kapel' v kuchevykh oblakah. *Tr. Gl. Geofiz. Obs.*, **19**, 122–132.